Supplement of The Cryosphere, 18, 475–488, 2024
https://doi.org/10.5194/tc-18-475-2024-supplement

The Cryosphere Open Access EGU

Supplement of

Cloud- and ice-albedo feedbacks drive greater Greenland Ice Sheet sensitivity to warming in CMIP6 than in CMIP5

Idunn Aamnes Mostue et al.

Correspondence to: Idunn Aamnes Mostue (idunnam@uio.no)

Simulation	Variable	Unit	Near-surface temperature anomaly (±std) (JJA) 5.4°C	(SON) 6.7°C
MAR CMIP5	ALB		-0.06 (± 0.002)	-0.008 (± 0.001)
MAR CMIP6	ALB		-0.062 (± 0.003)	-0.014 (± 0.001)
MAR CMIP5	CC	%	2.4 (± 0.9)	2.9 (± 0.8)
MAR CMIP6	CC	%	-2.2 (± 1.1)	-0.7 (± 0.9)
MAR CMIP5	COD		0.30 (± 0.02)	0.08 (± 0.01)
MAR CMIP6	COD		0.30 (± 0.03)	0.10 (± 0.01)
MAR CMIP5	LW_{net}	Wm^{-2}	6.8 (± 0.8)	2.5 (± 0.4)
MAR CMIP6	LW_{net}	Wm^{-2}	4.4 (± 1.1)	1.5 (± 0.5)
MAR CMIP5	LWD	Wm^{-2}	29.2 (± 1.0)	27.9 (± 0.4)
MAR CMIP6	LWD	Wm^{-2}	26.8 (± 0.9)	27.1 (± 0.5)
MAR CMIP5	LWU	Wm^{-2}	-22.4 (± 0.2)	-25.4 (± 0.1)
MAR CMIP6	LWU	Wm^{-2}	-22.2 (± 0.2)	-25.4 (± 0.1)
MAR CMIP5	ME	Gt/season	422.9 (± 9.5)	27.4 (± 2.7)
MAR CMIP6	ME	Gt/season	435.8 (± 15.0)	44.9 (± 7.1)
MAR CMIP5	Net_{rad}	Wm^{-2}	16.4 (± 0.5)	2.7 (± 0.3)
MAR CMIP6	Net_{rad}	Wm^{-2}	16.5 (± 0.9)	2.1 (± 0.5)
MAR CMIP5	RU	Gt/season	379.6 (± 12.8)	38.0 (± 3.6)
MAR CMIP6	RU	Gt/season	389.1 (± 18.6)	61.0 (± 8.5)
MAR CMIP5	SMB	Gt/season	-338.5(± 13.6)	-3.0 (± 6.1)
MAR CMIP6	SMB	Gt/season	-358.4 (± 18.0)	-27.7 (± 9.5)
MAR CMIP5	SW_{net}	Wm^{-2}	9.6 (± 0.9)	0.2 (± 0.1)
MAR CMIP6	SW_{net}	Wm^{-2}	12.1 (± 1.7)	0.6 (± 0.2)
MAR CMIP5	SWD	Wm^{-2}	-20.7 (± 2.0)	-2.5 (± 0.3)
MAR CMIP6	SWD	Wm^{-2}	-14.2 (± 1.8)	2.1 (± 0.5)

T 1: MAR CMIP5 and MAR CMIP6 projected anomalies of climate variables for a given temperature increase, associated units, and ± one standard deviation given in brackets. The standard deviation is calculated for a 20 year interval prior the selected warming. Temperature increase of + 5.4°C + 6.7°C is selected for summer (JJA) and autumn (SON) respectively, representing the close to end temperature for the MAR CMIP5 projections where it deviates the most from MAR CMIP6.

Forcing Field	JJA	SON
ACCESS1.3	(2078 – 2097)	(2069 – 2080)
CSIRO-Mk3-6-0	(2081 – 2100)	(2078 – 2097)
HadGEM2-ES	(2056 – 2075)	(2042 – 2061)
IPSL-CM5A-MR	(2056 – 2075)	(2045 – 2064)
MIROC5	(2060 – 2079)	(2057 – 2076)
NorESM1-M	(2069 – 2080)	(2065 – 2084)
CESM2	(2045 – 2064)	(2052 – 2071)
CNRM-CM6-1	(2060 – 2079)	(2056 – 2075)
CNRM-ESM2-1	(2062 – 2081)	(2059 – 2078)
MRI-ESM2-0	(2066 – 2085)	(2051 – 2070)
UKESM1-0-LL	(2030 – 2049)	(2032 – 2051)

T 2: Twenty-year warming period of $\sim 4°$C near-surface temperature, spatially averaged over the Greenland ice sheet for summer (JJA) and autumn (SON), from individual MAR simulations of CMIP5 models (top six models) and CMIP6 (bottom five models). All anomalies are related to the thirty-years averaged reference period (1961-1990).

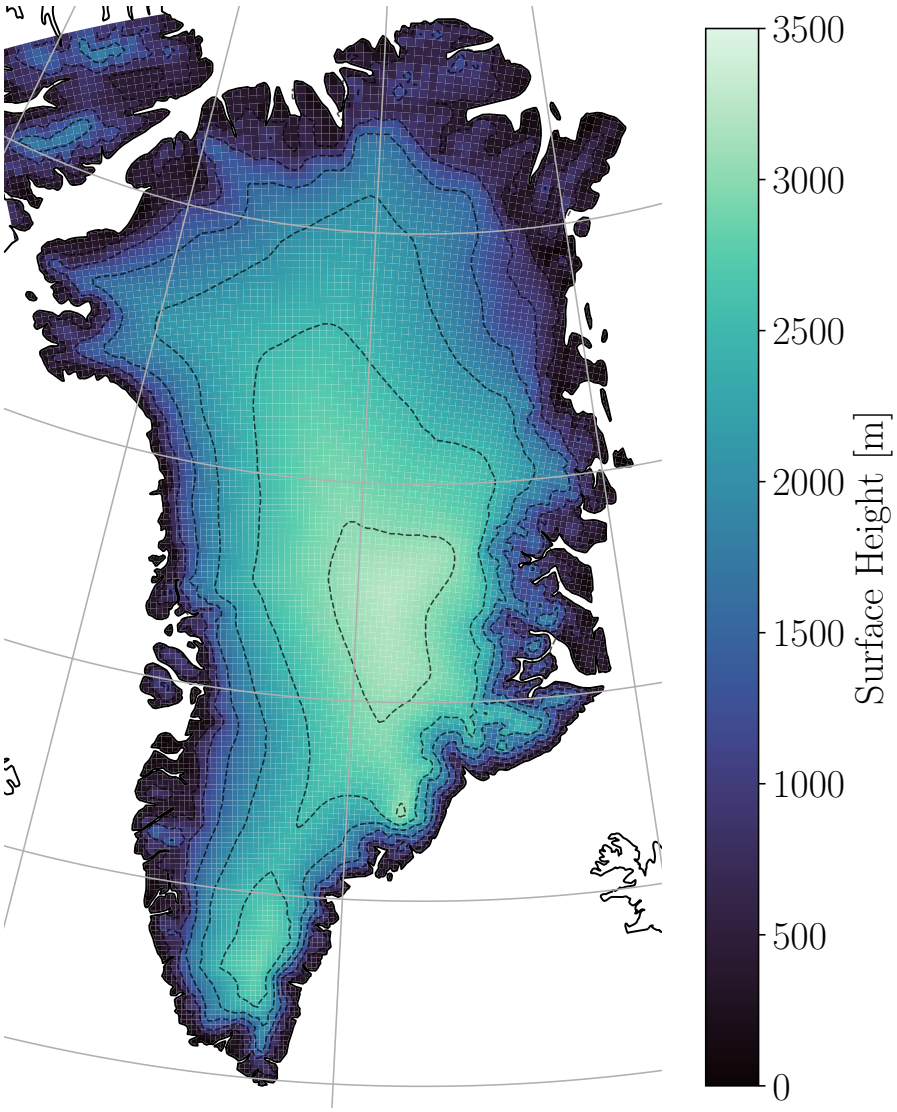

S 1: 15 km horizontal integration domain, and surface height over Greenland projected by the MAR simulations Dashed lines indicate elevation curves running from 500 - 3500 masl. with 500 m interval.

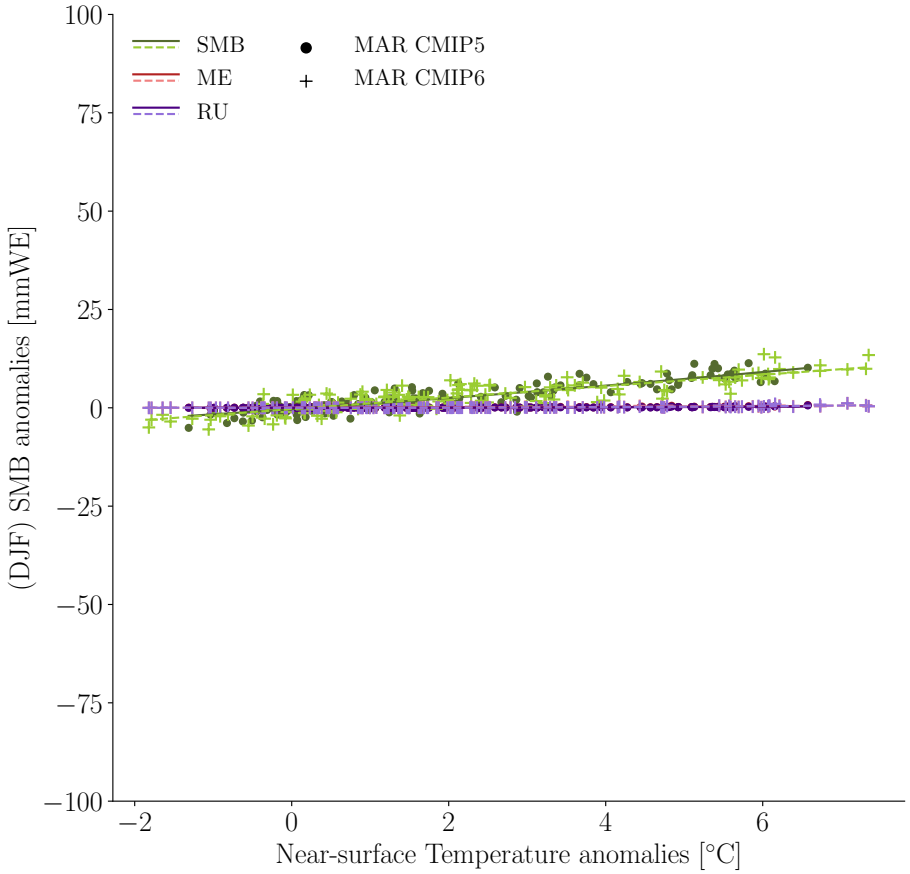

S 2: Seasonal SMB, melt and runoff anomalies [mmWE] over the GrIS according to near-surface temperature anomalies [°C]. Winter (DJF) SMB-, melt- (ME), and runoff anomalies (RU) [mmWE] over the GrIS as a function of annual near-surface temperature anomalies [°SC] from MAR CMIP5 (dots) and MAR CMIP6 (crosses), with regression drawn in solid lines for MAR CMIP5 and dashed lines for MAR CMIP6. All anomalies are related to the thirty-years averaged reference period (1961–1990)

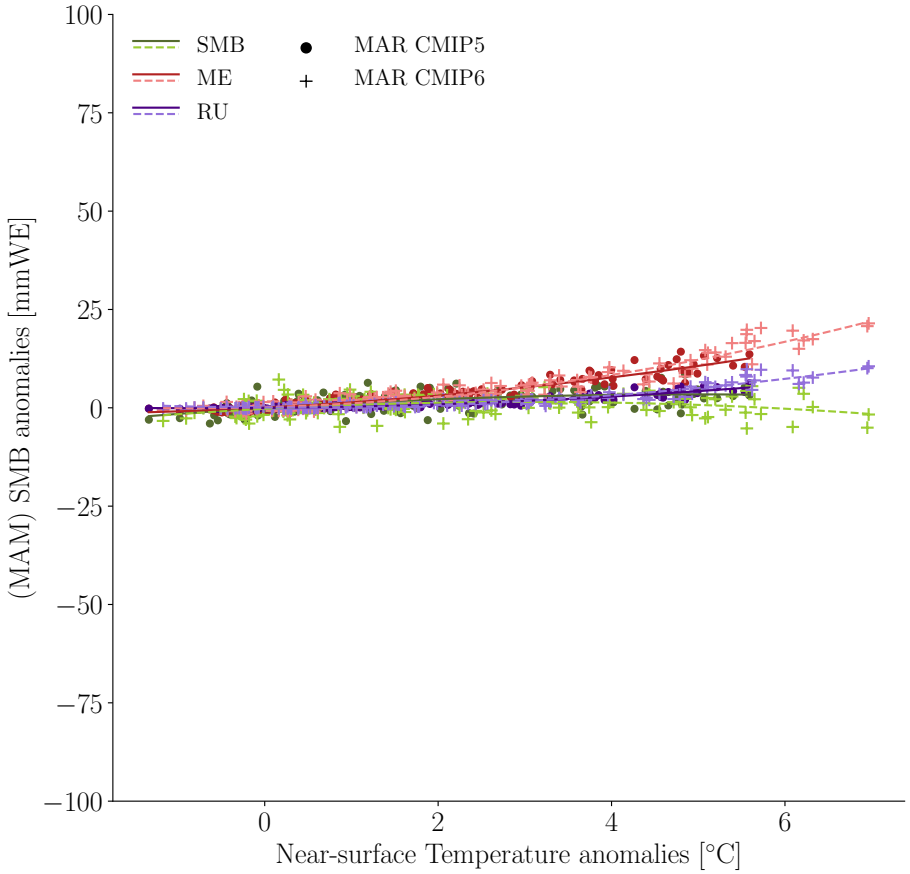

S 3: Seasonal SMB, melt and runoff anomalies [mmWE] over the GrIS according to near-surface temperature anomalies [°C]. Spring (MAM) SMB, melt (ME), and runoff anomalies (RU) [mmWE] over the GrIS as a function of annual near-surface temperature anomalies [°C] from MAR CMIP5 (dots) and MAR CMIP6 (crosses), with regression drawn in solid lines for MAR CMIP5 and dashed lines for MAR CMIP6. All anomalies are related to the thirty-years averaged reference period (1961–1990).

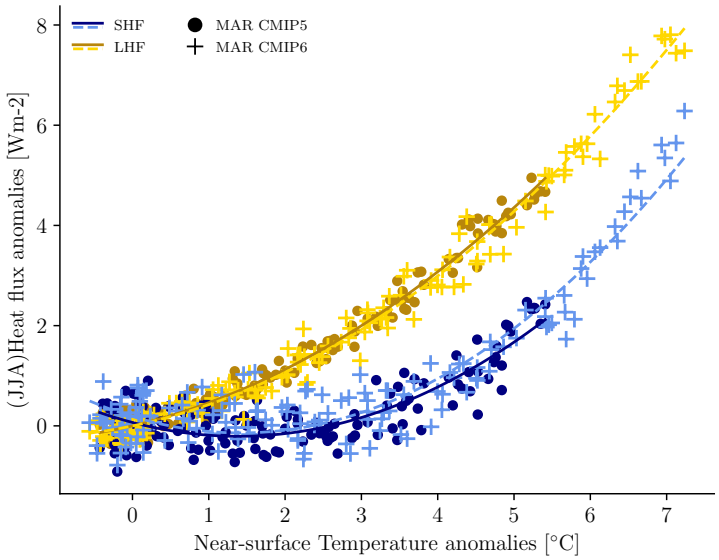

(a)

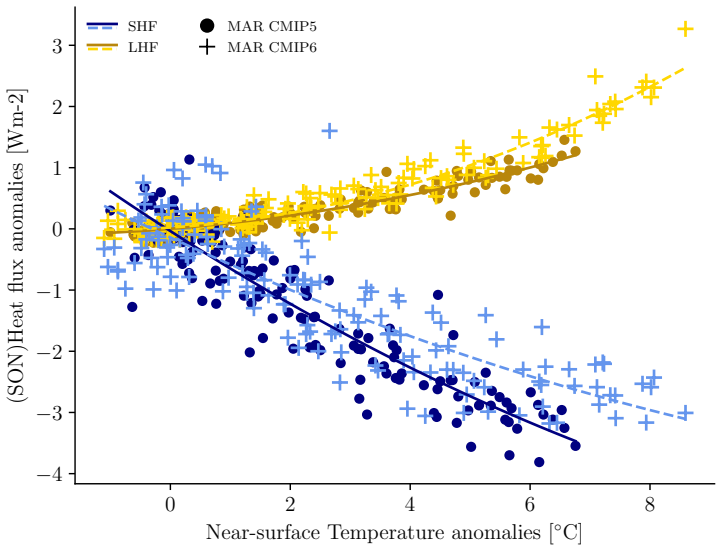

(b)

S 4: Seasonal Sensible - (SHF) and Latent heat flux (LHF) anomalies [Wm^{-2}] as a function of near-surface temperature anomalies [°C]. a) Summer (JJA) Sensible - (SHF) and Latent heat flux anomalies (LHF) [Wm^{-2}] over the GrIS as a function of near-surface temperature anomalies [°C] from MAR CMIP5 (dots) and MAR CMIP6 (crosses), with regression drawn in solid lines for MAR CMIP5 and dashed lines for MAR CMIP6. All anomalies are related to the thirty-year averaged reference period (1961-1990). **b)** Same as **a)**, but for autumn (SON).

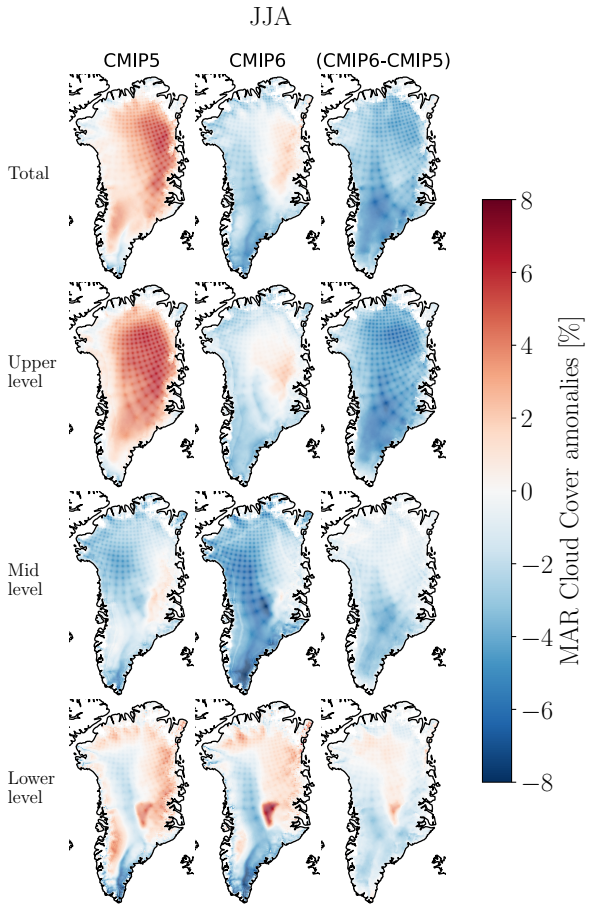

S 5: Spatial projection of Cloud cover anomalies [%] for MAR CMIP5 and MAR CMIP6 simulations (+ 4 °C ± 10 years) for summer (JJA). Twenty-year average (4 °C ± 10 years) of the cloud cover [%] over the GrIS) for summer (JJA). The four rows from top-down indicate the total, upper level (< 440 hPa), mid level ($\leqslant$ 680 hPa, $\geqslant$ 440 hPa), and lower level cloud cover (> 680 hPa). The three columns from left to right indicate the cloud cover anomalies for MAR CMIP5, for MAR CMIP6, and for the difference between the two (CMIP6-CMIP5). For MAR CMIP5 and MAR CMIP6 a positive value (red) indicates an increase in cloud cover, and a negative value (blue) a reduction in cloud cover compared to the reference period. For the difference (CMIP6-CMIP5) a positive value (red) indicates more positive cloud cover anomaly, and negative values (blue) indicate a more negative cloud cover anomaly in MAR CMIP6 compared to MAR CMIP5.

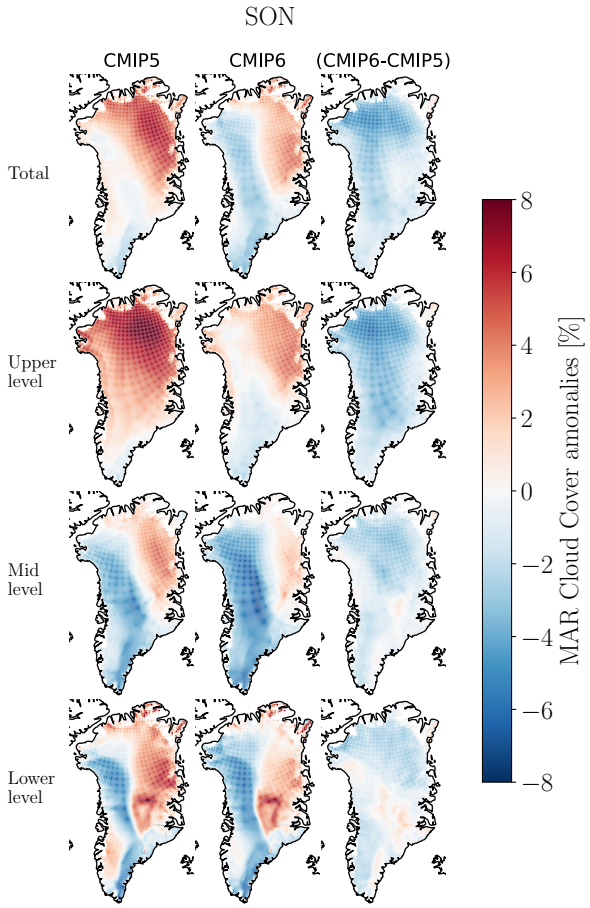

S 6: Spatial projection of Cloud cover anomalies [%] for MAR CMIP5 and MAR CMIP6 simulations (+ 4 °C ± 10 years) for autumn (SON). Twenty-year average (4 °C ± 10 years) of the cloud cover [%] over the GrIS) for autumn (SON). The four rows from top-down indicate the total, upper level (< 440 hPa), mid level ($\leqslant$ 680 hPa, $\geqslant$ 440 hPa), and lower level cloud cover (> 680 hPa). The three columns from left to right indicate the cloud cover anomalies for MAR CMIP5, for MAR CMIP6, and for the difference between the two (CMIP6-CMIP5). For MAR CMIP5 and MAR CMIP6 a positive value (red) indicates an increase in cloud cover, and a negative value (blue) a reduction in cloud cover compared to the reference period. For the difference (CMIP6-CMIP5) a positive value (red) indicates more positive cloud cover anomaly, and negative values (blue) indicate a more negative cloud cover anomaly in MAR CMIP6 compared to MAR CMIP5.

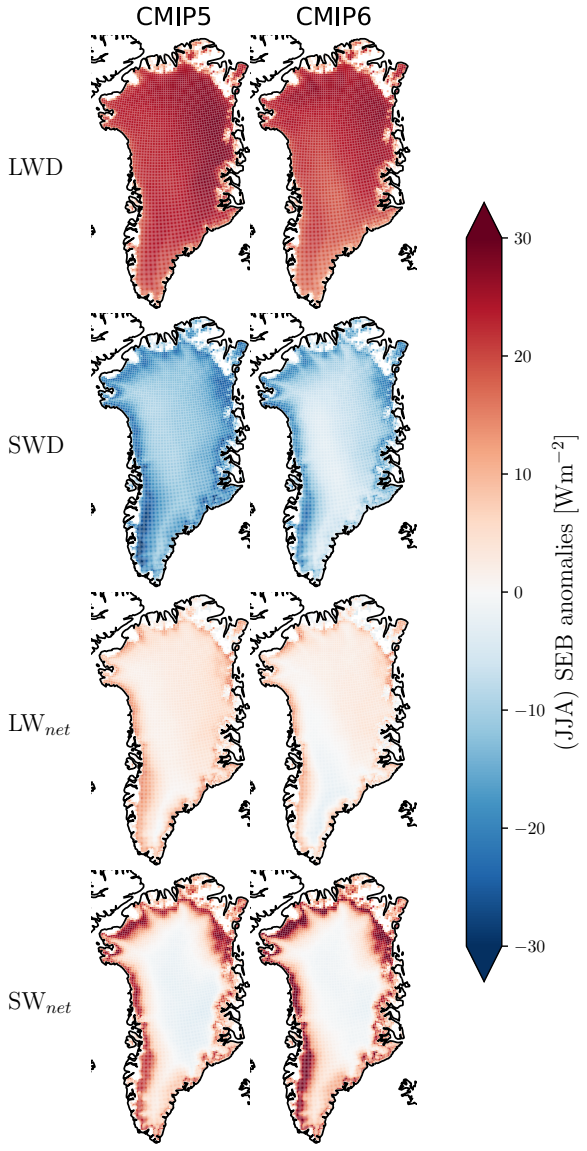

S 7: Spatial projection of selected SEB components anomaly for MAR CMIP5 and MAR CMIP6 simulations (+ 4°C ± 10 years) for summer (JJA). Twenty-year average (+ 4°C ± 10 years) anomalies of LWD, SWD, LW$_{net}$ and SW$_{net}$ [Wm^{-2}], of MAR CMIP5 (left) and MAR CMIP6 (right). Anomalies are related to the reference period (1961–1990). Positive value (red) indicates an incrFease in the energy flux reaching the surface, and a negative value (blue) a decrease, compared to the reference period (1961–1990).

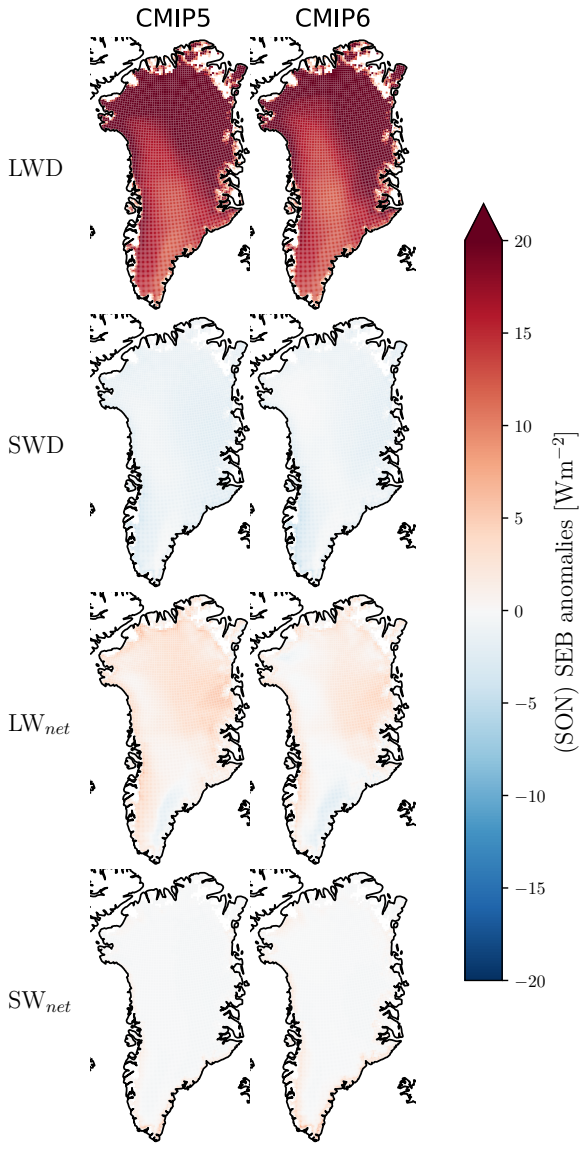

S 8: Spatial projection of selected SEB components anomaly for MAR CMIP5 and MAR CMIP6 simulations (+ 4°C ± 10 years) for autumn (SON). Twenty-year average (+ 4°C ± 10 years) anomalies of LWD, SWD, LW$_{net}$ and SW$_{net}$ [Wm^{-2}], of MAR CMIP5 (left) and MAR CMIP6 (right). Anomalies are related to the reference period (1961–1990). Positive value (red) indicates an increase in the energy flux reaching the surface, and a negative value (blue) a decrease, compared to the reference period (1961–1990).

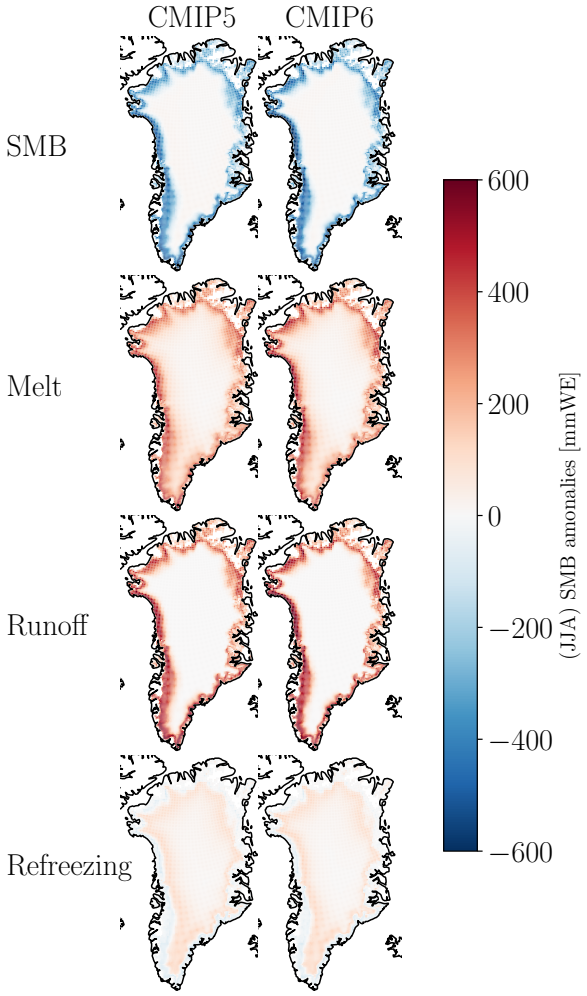

S 9: Spatial projection of selected SMB components anomaly for MAR CMIP5 and MAR CMIP6 simulations (+ 4°C ± 10 years) for summer (JJA). Twenty-year average (+ 4°C ± 10 years) anomalies of melt, runoff, refreezing and the total SMB [mmWE], of MAR CMIP5 (left) and MAR CMIP6 (right). Anomalies are related to the reference period (1961–1990). Positive value (red) indicates an increase in the surface mass balance components, and a negative value (blue) a decrease, compared to the reference period (1961–1990).

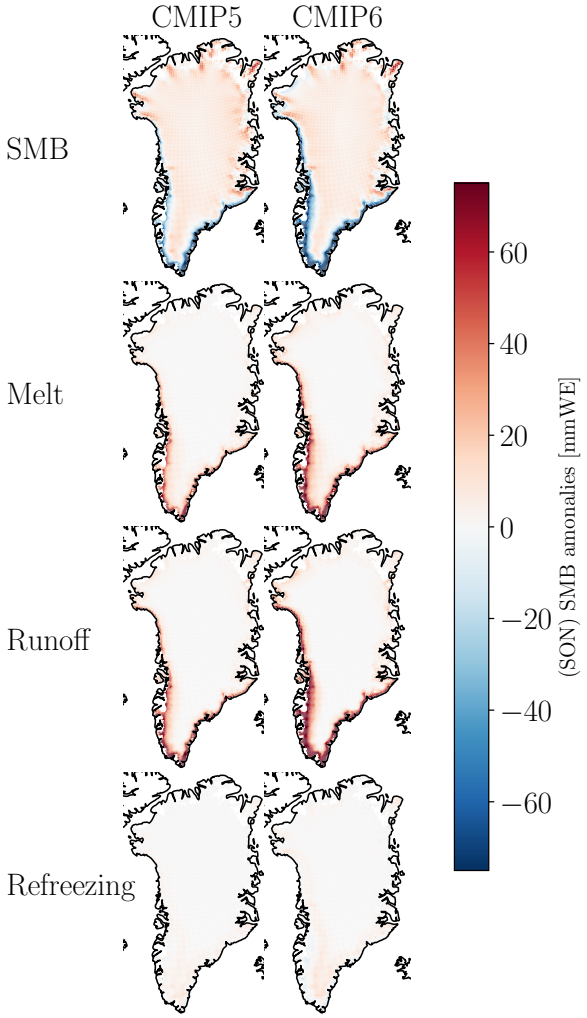

S 10: Spatial projection of selected SMB components anomaly for MAR CMIP5 and MAR CMIP6 simulations (+ 4°C ± 10 years) for autumn (SON). Twenty-year average (+ 4°C ± 10 years) anomalies of melt, runoff, refreezing and the total SMB [mmWE], of MAR CMIP5 (left) and MAR CMIP6 (right). Anomalies are related to the reference period (1961–1990). Positive value (red) indicates an increase in the surface mass balance components, and a negative value (blue) a decrease, compared to the reference period (1961–1990)

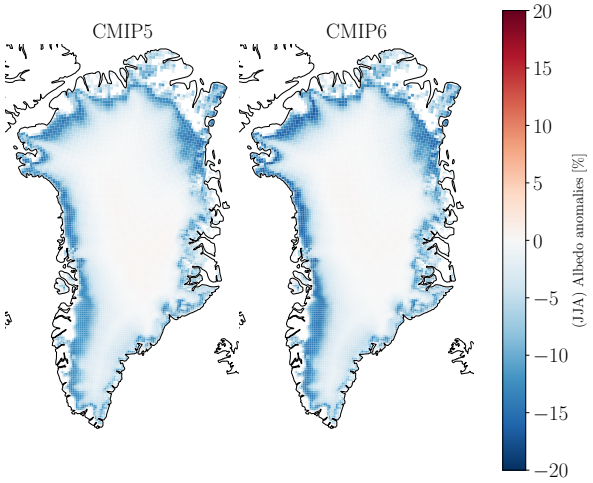

S 11: Spatial projection of albedo anomaly [%]for MAR CMIP5 and MAR CMIP6 simulations (+4° ± 10 years) for summer (JJA). Twenty-year average (+4° ± 10 years) of albedo [%] over the GrIS for summer (JJA). Anomalies are related to the reference period (1961–1990). Positive value (red) indicates an increase in the albedo, and a negative value (blue) a decrease, compared to the reference period (1961–1990).

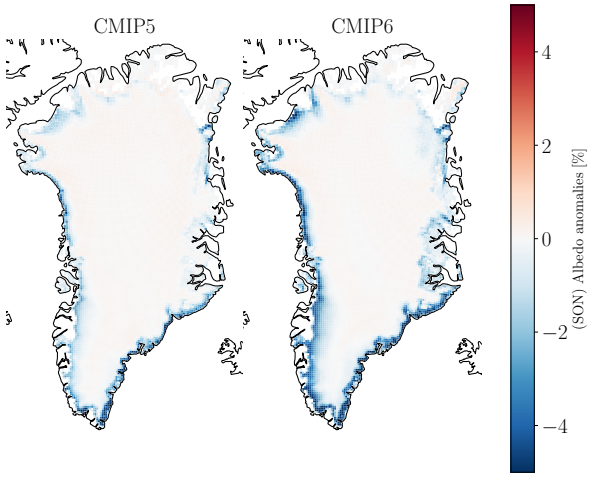

S 12: Spatial projection of albedo anomaly [%]for MAR CMIP5 and MAR CMIP6 simulations (+4° ± 10 years) for autumn (SON). Twenty-year average (+4° ± 10 years) of albedo [%] over the GrIS for autumn (SON). Anomalies are related to the reference period (1961–1990). Positive value (red) indicates an increase in the albedo, and a negative value (blue) a decrease, compared to the reference period (1961–1990).

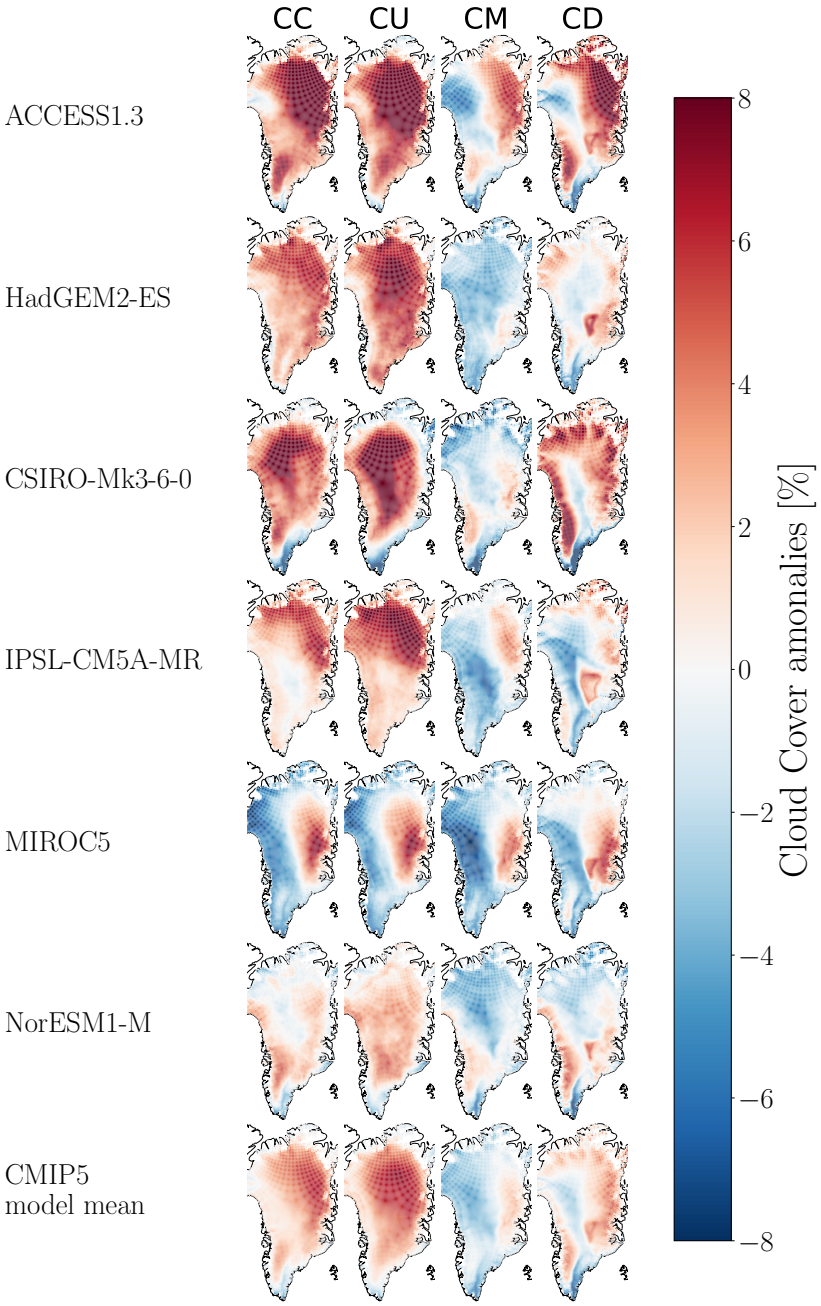

S 13: Spatial projection of Cloud cover anomalies [%] for individual MAR CMIP5 model simulations (+ 4 °C ± 10 years) for summer (JJA). Twenty-year average (+ 4 °C ± 10 years) of the total cloud cover (CC), upper-level cloud cover (CU, < 440 hPa), min-level cloud cover (CM, ⩾ 440 hPa, ⩽ 680 hPa), and low-level cloud cover (CD, > 680 hPa) [%] over the GrIS for the individual MAR CMIP5 model simulations and CMIP5 model mean for summer (JJA). A positive value (red) indicates an increase in cloud cover compared to the reference period, and a negative (blue) a reduction in cloud cover compare to the reference period.

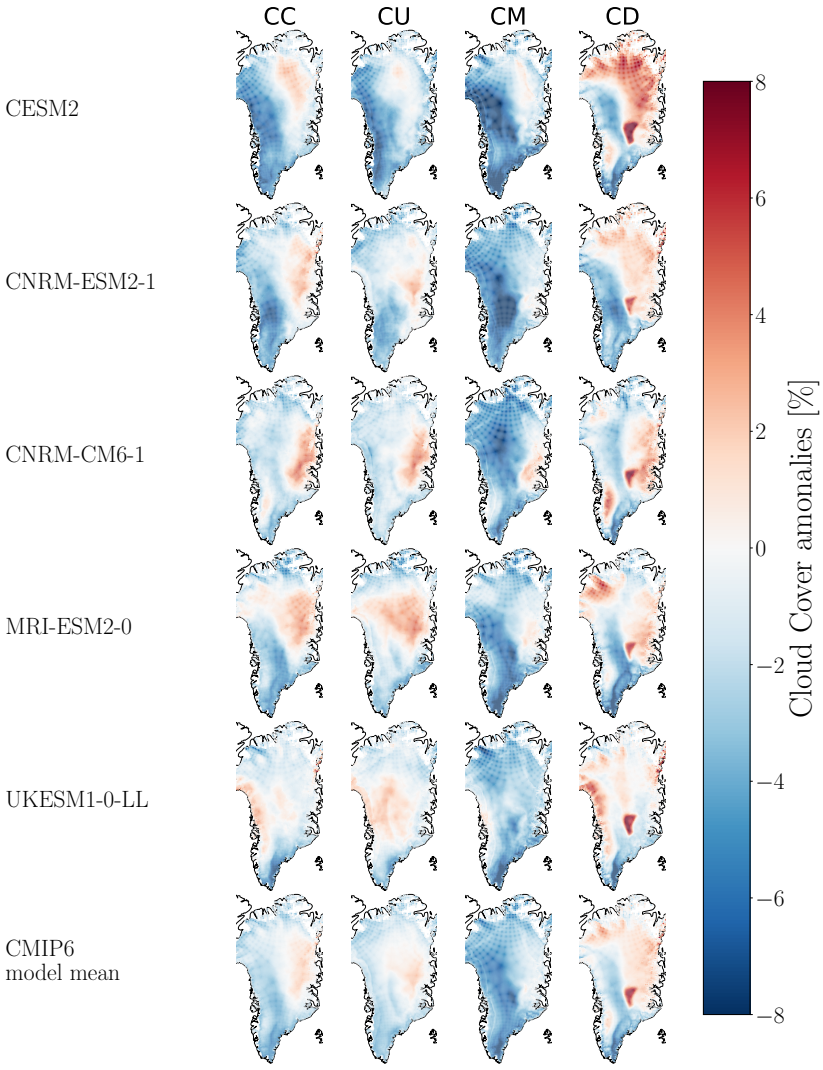

S 14: Spatial projection of Cloud cover anomalies [%] for individual MAR CMIP6 model simulations (+ 4 °C ± 10 years) for summer (JJA). Twenty-year average (+ 4 °C ± 10 years) of the total cloud cover (CC), upper-level cloud cover (CU, < 440 hPa), min-level cloud cover (CM, ⩾ 440 hPa, ⩽ 680 hPa), and low-level cloud cover (CD, > 680 hPa) [%] over the GrIS for the individual MAR CMIP6 model simulations and CMIP6 model mean for summer (JJA). A positive value (red) indicates an increase in cloud cover compared to the reference period, and a negative (blue) a reduction in cloud cover compare to the reference period.

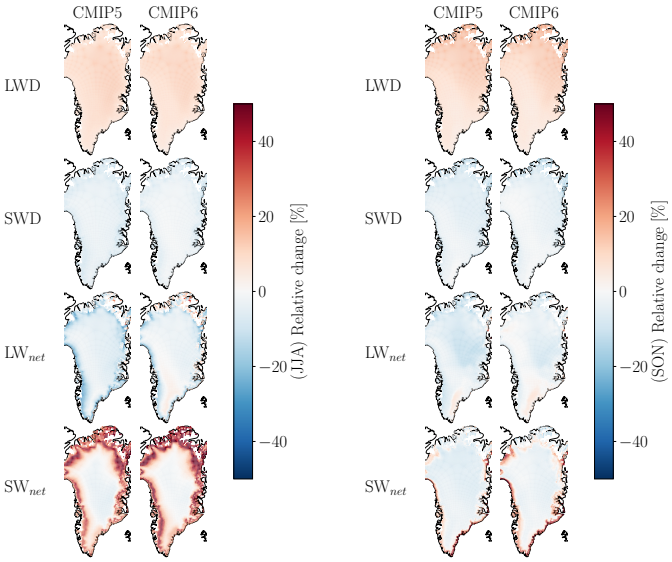

S 15: Relative change of SEB fluxes between MAR CMIP6 and MAR CMIP5 simulations (+ 4°C ± 10 years) for summer (JJA, left) and autumn (SON, right). Twenty-year average (+ 4°C ± 10 years) difference in SEB.

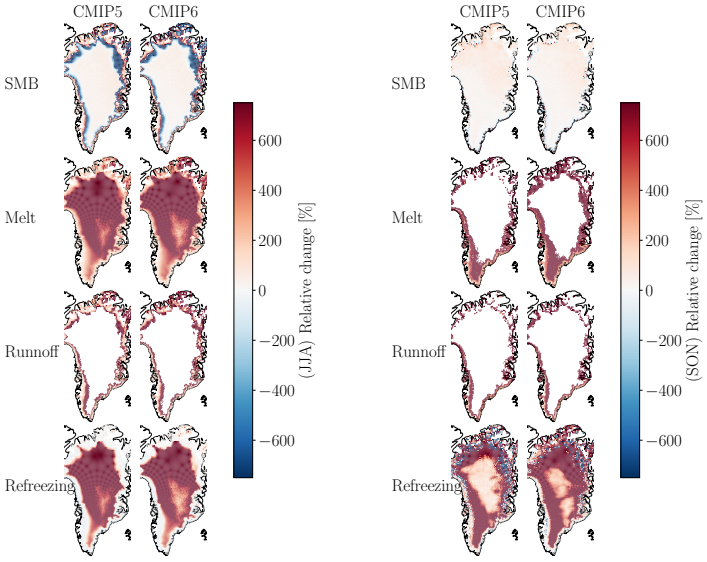

S 16: Relative change of selected SMB components of MAR CMIP6 and MAR CMIP5 simulations (+ 4°C ± 10 years) for summer (JJA, left) and autumn (SON, right). Twenty-year average (+ 4°C ± 10 years) relative change of melt, runoff, refreezing and the total SMB. Anomalies are related to the reference period (1961–1990)

Surface Energy Budget change and Cloud Cover change for the GrIS ablation- and accumulation zone

For this analysis we have separated the Surface Energy budget (SEB) change and the Cloud Cover change over the GrIS into the ablation zone and the accumulation zone of the GrIS.

This separation was done by creating a static mask for the ablation zone (accumulation zone) for all CMIP5 models and all CMIP6 models. The mask was created by first selecting an eleven-years period of 4°C annual warming for each of the eleven MAR simulations individually by creating a moving average, with a centred window of eleven-years over the near-surface time series. This allowed us to compute the arithmetic mean along the time series, where a eleven-years average for each year in the time series is returned. Then, by picking the year that returns a temperature closest to our designated near-surface temperature we found the eleven-years time interval for each model of similar averaged warming. Further, we use this annual warming period and define the ablation zone where SMB < 0 (accumulation zone SEB > 0) for all models in the CMIP5 ensemble and all models in the CMIP6 ensemble separately. Note that with this division we use the model ensemble ablation (accumulation) zone for only the grid cells where all models project ablation (accumulation) for CMIP5 and CMIP6 model ensemble individually. We then use our mask on the seasonal (JJA and SON) time-series of the SEB component anomalies and Cloud Cover anomalies, to create a separation for the ablation zone and the accumulation zone over the GrIS.

The summer (JJA) radiative SEB component anomalies [Wm^{-2}] and total cloud-cover anomalies [%] as a function of near-surface temperature anomalies [°C] over the GrIS ablation zone (left panel) and accumulation zone (right panel) are shown in Figure S17. Here we see that there is no difference in the Net radiative flux (grey) between MAR CMIP5 and MAR CMIP6. However, there is more LW_{net} coming from more LWD in MAR CMIP5. Further, we see more SWD reaching the surface in MAR CMIP6 compare MAR CMIP5, although the SW_{net} is similar between the two model ensembles, suggesting a higher albedo in MAR CMIP6 compared to MAR CMIP5. This behaviour can be explained by the cloud cover, where we have slight increasing cloud cover in MAR CMIP5, and decreasing cloud cover in MAR CMIP6 for a given temperature.

We see similar trends in the summer (JJA) accumulation zone, but of smaller magnitude in the SW radiative spectra. There is a stronger increase in cloud cover for MAR CMIP5 in the summer (JJA) accumulation compared to the ablation zone, and a slightly less reduction in cloud cover in CMIP6 compared to the ablation zone.

The autumn (SON) radiative SEB component anomalies [Wm^{-2}] and total cloud-cover anomalies [%] as a function of near-surface temperature anomalies [°C] over the GrIS ablation zone (left panel) and accumulation zone (right panel) are shown in Figure S18.

Here, we note no difference for the different SEB components between CMIP5 and CMIP6. We do however have differences in the cloud cover anomalies, with increasing cloud cover for a given near-surface temperature increase in MAR CMIP5 and decreasing in MAR CMIP6.

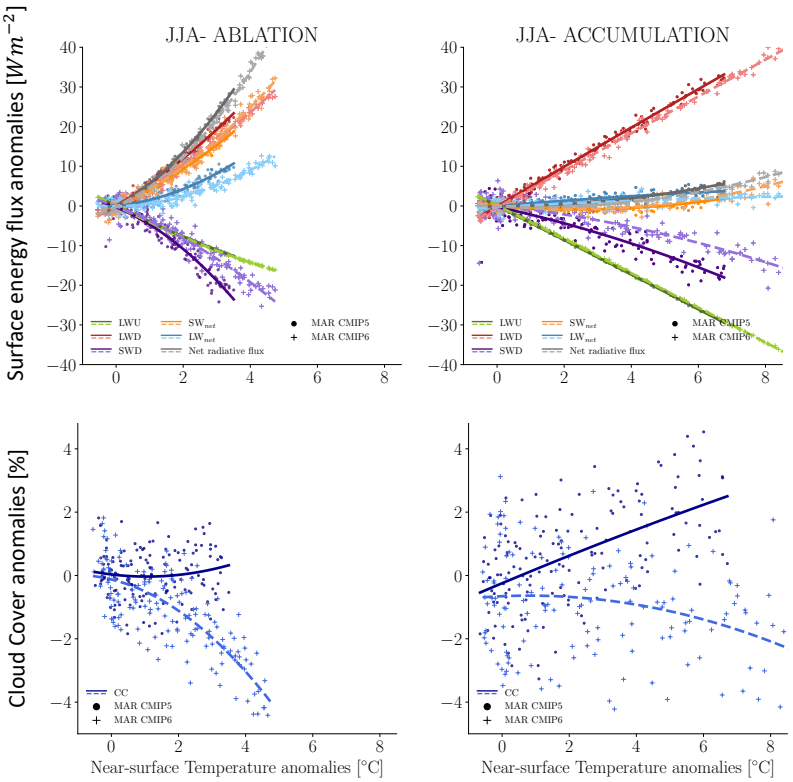

S 17: Radiative SEB component anomalies [Wm^{-2}] and total cloud cover anomalies [%] as a function of the near-surface air temperature anomalies [°C] over the GrIS ablation zone and accumulation zone. Seasonal (JJA) radiative SEB component anomalies [Wm^{-2}] (top panel) and cloud cover anomalies [%] (bottom panel) over the GrIS ablation zone (left panel) and accumulation zone (right panel) according to near-surface air temperature anomalies [°C] from MAR CMIP5 (dots) and MAR CMIP6 (crosses). Regression is drawn in solid lines for MAR CMIP5 and dashed lines for MAR CMIP6. The SEB components include the radiative energy fluxes of longwave down (LWD), longwave up (LWU), shortwave down (SWD), net longwave radiation (LW_{net}), net shortwave radiation (SW_{net}), and Net radiative flux. Positive direction towards the surface.

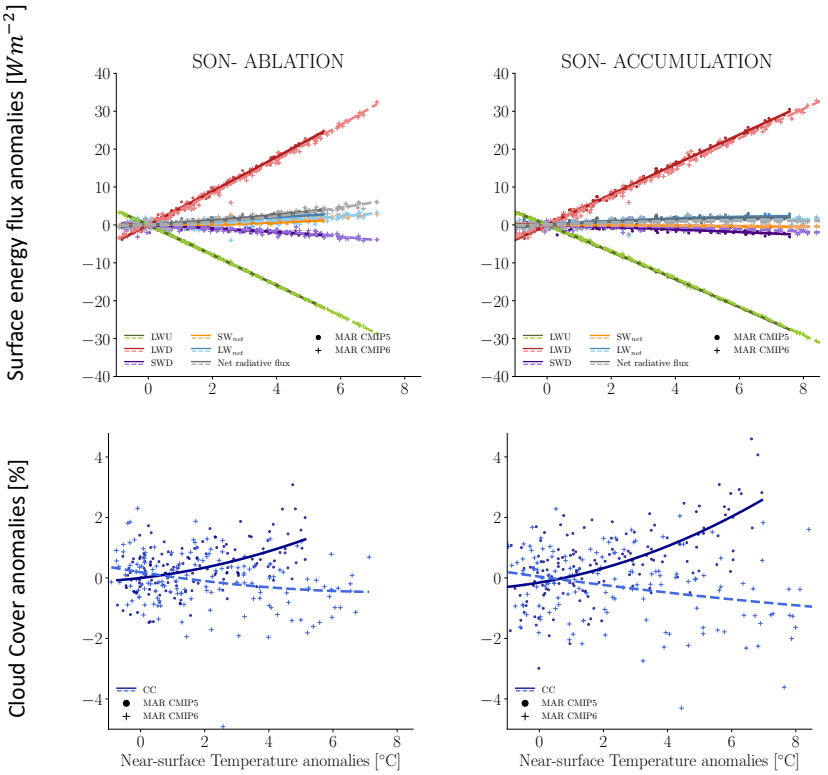

S 18: Radiative SEB component anomalies [$\mathbf{Wm^{-2}}$] and total cloud cover anomalies [%] as a function of the near-surface air temperature anomalies [°C] over the GrIS ablation zone and accumulation zone. Seasonal (SON) radiative SEB component anomalies [Wm^{-2}] (top panel) and cloud cover anomalies [%] (bottom panel) over the GrIS ablation zone (left panel) and accumulation zone (right panel) according to near-surface air temperature anomalies [°C] from MAR CMIP5 (dots) and MAR CMIP6 (crosses). Regression is drawn in solid lines for MAR CMIP5 and dashed lines for MAR CMIP6. The SEB components include the radiative energy fluxes of longwave down (LWD), longwave up (LWU), shortwave down (SWD), net longwave radiation (LW_{net}), net shortwave radiation (SW_{net}), and Net radiative flux. Positive direction towards the surface.